

## Hard-thermal-loop QCD Thermodynamics

Michael Strickland<sup>1,2</sup>, Jens O. Andersen<sup>3</sup>, Lars E. Leganger<sup>3</sup>, and Nan Su<sup>2</sup>

<sup>1</sup> *Department of Physics, Gettysburg College, Gettysburg, PA 17325, USA*

<sup>2</sup> *Frankfurt Institute for Advanced Studies, Ruth-Moufang-Str. 1, D-60438 Frankfurt am Main, Germany*

<sup>3</sup> *Department of Physics, Norwegian University of Science and Technology, Høgskoleringen 5, N-7491 Trondheim, Norway*

Naively resummed perturbative approximations to the thermodynamic functions of QCD do not converge at phenomenologically relevant temperatures. Here we review recent results of a three-loop hard-thermal-loop perturbation theory calculation of the thermodynamic functions of a quark-gluon plasma for general  $N_c$  and  $N_f$ . We show comparisons of our recent results with lattice data from both the hotQCD and Wuppertal-Budapest groups. We demonstrate that the three-loop hard-thermal-loop perturbation result for QCD thermodynamics agrees with lattice data down to temperatures  $T \sim 2T_c$ .

### §1. Introduction

A key question in the study of the quark-gluon plasma (QGP) is whether or not one can use a weakly-coupled framework to calculate properties of the system at temperatures near the QGP phase transition temperature,  $T_c \sim 170$  MeV. This is phenomenologically relevant because the ultrarelativistic heavy-ion collision experiments at Brookhaven National Labs (RHIC), and forthcoming at CERN (LHC) generate initial QGP temperatures which are on the order of  $2T_c$  and  $5T_c$ , respectively. At these temperatures the strong coupling constant is approximately  $\alpha_s = g_s^2/4\pi \sim 0.3$ . Unfortunately, this places the system in regime where the coupling is neither very small nor very large. Prior to experiments at RHIC, theorists expected that the QGP could be described in terms of weakly interacting quasiparticles; however, data from RHIC suggested that the state of matter created behaved more like a strongly coupled fluid with a small viscosity.<sup>1)</sup> This has inspired work on strongly-coupled formalisms based on e.g. the AdS/CFT correspondence. However, some observables such as jet quenching<sup>2)</sup> and elliptic flow<sup>3)</sup> can also be described using perturbative methods and so it is difficult to decide whether the plasma is strongly or weakly coupled based only on RHIC data.

In the upcoming heavy-ion collisions at LHC, the energy densities and therefore the initial temperatures will be higher than those achieved at RHIC. One expects initial temperatures on the order of  $5T_c$ . An important question is then whether the matter generated can be described in terms of weakly interacting quasiparticles at these higher temperatures. Lattice simulations of QCD provide a clean testing ground for the quasiparticle picture and in this proceedings report we compare recently obtained next-to-next-to-leading order (NNLO) results for thermodynamic functions of QCD<sup>4)</sup> with lattice data<sup>5),6)</sup> and with previous results at leading order (LO) and next-to-leading order (NLO).<sup>7)</sup> The calculations presented here

are based on the hard-thermal-loop perturbation theory (HTLpt) reorganization of finite-temperature perturbation theory. In HTLpt one expands around an ideal gas of massive gluonic and quark quasiparticles where screening effects and Landau damping are gauge-invariantly built in. Our results indicate that lattice data are consistent with a quasiparticle picture down to temperatures of  $T \sim 2T_c$ .

The free energy of QCD is now known up to order  $\alpha_s^3 \log \alpha_s$ .<sup>8),9)</sup> Unfortunately, a straightforward application of perturbation theory is of no quantitative use at phenomenologically relevant temperatures. The problem is that the weak-coupling expansion oscillates wildly and shows no sign of convergence unless the temperature is extremely high. For example, if one compares the  $g_s^3$ -contribution to the QCD free energy with three quark flavors to the  $g_s^2$ -contribution, the former is smaller only if  $\alpha_s \leq 0.07$ , which corresponds to  $T \sim 10^5$  GeV or  $T \sim 5 \times 10^5 T_c$ . There are several ways of reorganizing the perturbative series at finite temperature.<sup>10)</sup> These reorganizations are based on a quasiparticle picture where one is perturbing about an ideal gas of massive quasiparticles, rather than that of an ideal gas of massless quarks and gluons. In scalar  $\phi^4$ -theory the basic idea is to add and subtract a thermal mass term from the bare Lagrangian and to include the added piece in the free part of the Lagrangian. The subtracted piece is then treated as an interaction on the same footing as the quartic term.<sup>11)</sup> In gauge theories, however, simply adding and subtracting a local mass term, violates gauge invariance.<sup>12)</sup> Instead, one adds and subtracts an HTL improvement term, which dresses the propagators and vertices self-consistently so that the reorganization is manifestly gauge invariant.<sup>13)</sup>

## §2. Hard-thermal-loop perturbation theory

The Lagrangian density for an  $SU(N_c)$  Yang-Mills theory with  $N_f$  fermions in Minkowski space is

$$\mathcal{L}_{\text{QCD}} = -\frac{1}{2} \text{Tr} [G_{\mu\nu} G^{\mu\nu}] + i\bar{\psi} \gamma^\mu D_\mu \psi + \mathcal{L}_{\text{gf}} + \mathcal{L}_{\text{gh}} + \Delta\mathcal{L}_{\text{QCD}}, \quad (2.1)$$

where the field strength is  $G^{\mu\nu} = \partial^\mu A^\nu - \partial^\nu A^\mu - ig_s[A^\mu, A^\nu]$  and the covariant derivative is  $D^\mu = \partial^\mu - ig_s A^\mu$ .  $\Delta\mathcal{L}_{\text{QCD}}$  contains the counterterms necessary to cancel the ultraviolet divergences. The ghost term  $\mathcal{L}_{\text{gh}}$  depends on the gauge-fixing term  $\mathcal{L}_{\text{gf}}$ . In this paper we choose the class of covariant gauges where the gauge-fixing term is  $\mathcal{L}_{\text{gf}} = -\frac{1}{\xi} \text{Tr} [(\partial_\mu A^\mu)^2]$ . With the standard normalization, we have  $c_A = N_c$ ,  $d_A = N_c^2 - 1$ ,  $s_F = N_f/2$ ,  $d_F = N_c N_f$ , and  $s_{2F} = (N_c^2 - 1)N_f/4N_c$ .

Hard-thermal-loop perturbation theory is a reorganization of the perturbation series for thermal QCD. The Lagrangian density is written as

$$\mathcal{L} = (\mathcal{L}_{\text{QCD}} + \mathcal{L}_{\text{HTL}}) \Big|_{g_s \rightarrow \sqrt{\delta} g_s} + \Delta\mathcal{L}_{\text{HTL}}, \quad (2.2)$$

where  $\Delta\mathcal{L}_{\text{HTL}}$  contains the additional counterterms necessary to cancel the ultraviolet divergences introduced by HTLpt. The HTL improvement term is

$$\mathcal{L}_{\text{HTL}} = -\frac{1}{2}(1-\delta)m_D^2 \text{Tr} \left( G_{\mu\alpha} \left\langle \frac{y^\alpha y^\beta}{(y \cdot D)^2} \right\rangle_y G^\mu{}_\beta \right) + (1-\delta) im_q^2 \bar{\psi} \gamma^\mu \left\langle \frac{y^\mu}{y \cdot D} \right\rangle_y \psi, \quad (2.3)$$

where  $y^\mu = (1, \hat{\mathbf{y}})$  is a light-like four-vector, and  $\langle \dots \rangle_{\hat{\mathbf{y}}}$  represents the average over the directions of  $\hat{\mathbf{y}}$ . The free parameters  $m_D$  and  $m_q$  are identified with the Debye screening mass and the fermion thermal mass, respectively. The parameter  $\delta$  is a formal expansion parameter and bookkeeping device: HTLpt is defined as an expansion in powers of  $\delta$  around  $\delta = 0$ . This expansion generates systematically dressed propagators and vertices. It also automatically generates new higher-order terms that ensure that there is no overcounting of Feynman diagrams. We emphasize that HTLpt is gauge invariant at each order in  $\delta$ .

The HTL perturbative expansion generates new divergences. We use  $\overline{\text{MS}}$  dimensional regularization with a renormalization scale  $\mu$  to regularize infrared and ultraviolet divergences. There is no rigorous proof that HTLpt is renormalizable, so the general structure of the counterterms is unknown. However, one can show that through NNLO, HTLpt can be renormalized using only local counterterms for the vacuum, the Debye and fermion masses, and the coupling constant. The counterterm for  $\alpha_s$  coincides with the perturbative value giving rise to the standard one-loop running. We do not list the counterterms here, but present the full results elsewhere.<sup>14)</sup> If the expansion in  $\delta$  could be carried out to all orders, the final result would be independent of the HTL parameters  $m_D$  and  $m_q$ . However, at any finite order in  $\delta$ , the results depend on  $m_D$  and  $m_q$ . A prescription is then required to determine these parameters. We will discuss the prescription we use below.

### §3. Thermodynamic potential

In this section, we present the final results for the thermodynamic potential  $\Omega$  at orders  $\delta^0$  (LO),  $\delta$  (NLO), and  $\delta^2$  (NNLO). The LO and NLO results were first obtained previously<sup>7)</sup> and they are listed here for completeness. At LO, the thermodynamic potential was calculated exactly, while at NLO and NNLO the resulting expressions for the diagrams are too complicated. To make the calculations tractable, the thermodynamic potential is therefore evaluated approximately by expanding them in powers of  $m_D/T$  and  $m_q/T$  which assumes that these ratios are  $\mathcal{O}(g_s)$ . This implies that the thermodynamic potential is evaluated in a double expansion in  $g_s$ ,  $m_D/T$ , and  $m_q/T$ , and we have kept terms that contribute naively through order  $g_s^5$ . Due to the magnetic mass problem,<sup>15)</sup> HTLpt suffers from the same infrared divergences as ordinary perturbation theory and  $g_s^5$  is the highest order computable using only perturbative methods.

The complete expression for the leading order thermodynamic potential is given by<sup>7)</sup>

$$\begin{aligned} \frac{\Omega_{\text{LO}}}{\mathcal{F}_{\text{ideal}}} = & 1 + \frac{7}{4} \frac{d_F}{d_A} - \frac{15}{2} \hat{m}_D^2 - 30 \frac{d_F}{d_A} \hat{m}_q^2 + 30 \hat{m}_D^3 + \frac{45}{4} \left( \log \frac{\hat{\mu}}{2} - \frac{7}{2} + \gamma_E + \frac{\pi^2}{3} \right) \hat{m}_D^4 \\ & - 60 \frac{d_F}{d_A} (\pi^2 - 6) \hat{m}_q^4, \end{aligned} \quad (3.1)$$

where  $\mathcal{F}_{\text{ideal}} = -(N_c^2 - 1)\pi^2 T^4/45$  is the free energy of an ideal gas of noninteracting gluons and  $\gamma_E$  is the Euler-Mascheroni constant. Moreover, we have introduced the dimensionless parameters  $\hat{\mu} = \mu/2\pi T$ ,  $\hat{m}_D = m_D/2\pi T$ , and  $\hat{m}_q = m_q/2\pi T$ .

The NLO thermodynamic potential reads<sup>7)</sup>

$$\begin{aligned}
\frac{\Omega_{\text{NLO}}}{\mathcal{F}_{\text{ideal}}} &= 1 + \frac{7 d_F}{4 d_A} - 15 \hat{m}_D^3 - \frac{45}{4} \left( \log \frac{\hat{\mu}}{2} - \frac{7}{2} + \gamma_E + \frac{\pi^2}{3} \right) \hat{m}_D^4 + 60 \frac{d_F}{d_A} (\pi^2 - 6) \hat{m}_q^4 \\
&+ \frac{c_A \alpha_s}{3\pi} \left[ -\frac{15}{4} + 45 \hat{m}_D - \frac{165}{4} \left( \log \frac{\hat{\mu}}{2} - \frac{36}{11} \log \hat{m}_D - 2.001 \right) \hat{m}_D^2 \right. \\
&+ \left. \frac{495}{2} \left( \log \frac{\hat{\mu}}{2} + \frac{5}{22} + \gamma_E \right) \hat{m}_D^3 \right] \\
&+ \frac{s_F \alpha_s}{\pi} \left[ -\frac{25}{8} + 15 \hat{m}_D + 5 \left( \log \frac{\hat{\mu}}{2} - 2.33452 \right) \hat{m}_D^2 \right. \\
&- 30 \left( \log \frac{\hat{\mu}}{2} - \frac{1}{2} + \gamma_E + 2 \log 2 \right) \hat{m}_D^3 \\
&\left. - 45 \left( \log \frac{\hat{\mu}}{2} + 2.19581 \right) \hat{m}_q^2 + 180 \hat{m}_D \hat{m}_q^2 \right]. \tag{3.2}
\end{aligned}$$

Finally, our new result for the NNLO thermodynamic potential for QCD is

$$\begin{aligned}
\frac{\Omega_{\text{NNLO}}}{\mathcal{F}_{\text{ideal}}} &= 1 + \frac{7 d_F}{4 d_A} - \frac{15}{4} \hat{m}_D^3 \\
&+ \frac{c_A \alpha_s}{3\pi} \left[ -\frac{15}{4} + \frac{45}{2} \hat{m}_D - \frac{135}{2} \hat{m}_D^2 - \frac{495}{4} \left( \log \frac{\hat{\mu}}{2} + \frac{5}{22} + \gamma_E \right) \hat{m}_D^3 \right] \\
&+ \frac{s_F \alpha_s}{\pi} \left[ -\frac{25}{8} + \frac{15}{2} \hat{m}_D + 15 \left( \log \frac{\hat{\mu}}{2} - \frac{1}{2} + \gamma_E + 2 \log 2 \right) \hat{m}_D^3 - 90 \hat{m}_q^2 \hat{m}_D \right] \\
&+ \left( \frac{c_A \alpha_s}{3\pi} \right)^2 \left[ \frac{45}{4} \frac{1}{\hat{m}_D} - \frac{165}{8} \left( \log \frac{\hat{\mu}}{2} - \frac{72}{11} \log \hat{m}_D - \frac{84}{55} - \frac{6}{11} \gamma_E \right. \right. \\
&\left. \left. - \frac{74}{11} \frac{\zeta'(-1)}{\zeta(-1)} + \frac{19}{11} \frac{\zeta'(-3)}{\zeta(-3)} \right) + \frac{1485}{4} \left( \log \frac{\hat{\mu}}{2} - \frac{79}{44} + \gamma_E + \log 2 - \frac{\pi^2}{11} \right) \hat{m}_D \right] \\
&+ \left( \frac{c_A \alpha_s}{3\pi} \right) \left( \frac{s_F \alpha_s}{\pi} \right) \left[ \frac{15}{2} \frac{1}{\hat{m}_D} - \frac{235}{16} \left( \log \frac{\hat{\mu}}{2} - \frac{144}{47} \log \hat{m}_D \right. \right. \\
&\left. \left. - \frac{24}{47} \gamma_E + \frac{319}{940} + \frac{111}{235} \log 2 - \frac{74}{47} \frac{\zeta'(-1)}{\zeta(-1)} + \frac{1}{47} \frac{\zeta'(-3)}{\zeta(-3)} \right) \right. \\
&+ \left. \frac{315}{4} \left( \log \frac{\hat{\mu}}{2} - \frac{8}{7} \log 2 + \gamma_E + \frac{9}{14} \right) \hat{m}_D + 90 \frac{\hat{m}_q^2}{\hat{m}_D} \right] + \left( \frac{s_F \alpha_s}{\pi} \right)^2 \left[ \frac{5}{4} \frac{1}{\hat{m}_D} \right. \\
&+ \frac{25}{12} \left( \log \frac{\hat{\mu}}{2} + \frac{1}{20} + \frac{3}{5} \gamma_E - \frac{66}{25} \log 2 + \frac{4}{5} \frac{\zeta'(-1)}{\zeta(-1)} - \frac{2}{5} \frac{\zeta'(-3)}{\zeta(-3)} \right) \\
&\left. - 15 \left( \log \frac{\hat{\mu}}{2} - \frac{1}{2} + \gamma_E + 2 \log 2 \right) \hat{m}_D + 30 \frac{\hat{m}_q^2}{\hat{m}_D} \right] \\
&+ s_{2F} \left( \frac{\alpha_s}{\pi} \right)^2 \left[ \frac{15}{64} (35 - 32 \log 2) - \frac{45}{2} \hat{m}_D \right], \tag{3.3}
\end{aligned}$$

where  $\zeta(z)$  is the Riemann zeta-function.

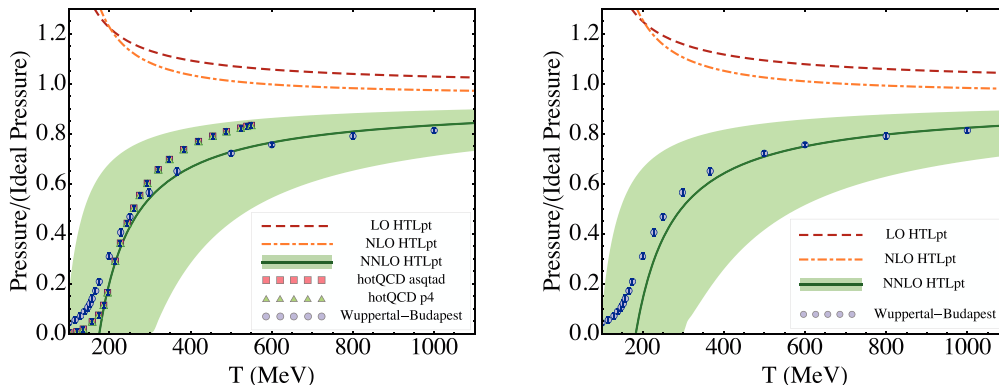


Fig. 1. Comparison of LO, NLO, and NNLO predictions for the scaled pressure for  $N_f = 2 + 1$  (left panel) and  $N_f = 2 + 1 + 1$  (right panel) with lattice data from Cheng et al.<sup>5)</sup> and Borsanyi et al.<sup>6)</sup> We use  $N_c = 3$ , three-loop running for  $\alpha_s$ ,  $\mu = 2\pi T$ , and  $\Lambda_{\overline{\text{MS}}} = 344$  MeV. Shaded band shows the result of varying the renormalization scale  $\mu$  by a factor of two around  $\mu = 2\pi T$  for the NNLO result. See main text for details.

As pointed out earlier, the HTL mass parameters are completely arbitrary and we need a prescription for them in order to complete a calculation. The variational mass prescription unfortunately gives rise to a complex Debye mass and  $m_q = 0$  at NNLO. One strategy is therefore to throw away the imaginary part of the thermodynamic potential to obtain thermodynamic functions that are real valued.<sup>16), 17)</sup> Here we use another strategy explored in Refs. 16), 17) that is inspired by dimensional reduction: We equate the Debye mass with the mass parameter of three-dimensional electric QCD (EQCD),<sup>9)</sup> i.e.  $m_D = m_E$ . In Ref. 9), it was calculated to NLO giving

$$m_D^2 = \frac{4\pi\alpha_s}{3}T^2 \left\{ c_A + s_F + \frac{c_A^2\alpha_s}{3\pi} \left( \frac{5}{4} + \frac{11}{2}\gamma_E + \frac{11}{2}\log\frac{\hat{\mu}}{2} \right) + \frac{c_A s_F \alpha_s}{\pi} \left[ \frac{3}{4} - \frac{4}{3}\log 2 + \frac{7}{6} \left( \gamma_E + \log\frac{\hat{\mu}}{2} \right) \right] + \frac{s_F^2\alpha_s}{\pi} \left( \frac{1}{3} - \frac{4}{3}\log 2 - \frac{2}{3}\gamma_E - \frac{2}{3}\log\frac{\hat{\mu}}{2} \right) - \frac{3}{2}\frac{s_{2F}\alpha_s}{\pi} \right\}. \quad (3.4)$$

This mass can be interpreted as the contribution to the Debye mass from the hard scale  $T$  and is well defined and gauge invariant order-by-order in perturbation theory. However, beyond NLO, it will also depend on factorization scale that separates the hard scale and the soft scale  $gT$ . For the quark mass, here we choose  $m_q = 0$ .

The final NNLO results are very insensitive to whether one chooses a perturbative mass prescription for  $m_q$  or  $m_q = 0$ ; however, convergence is improved with the choice  $m_q = 0$ . A detailed presentation of the full calculation of the NNLO thermodynamic potential and the dependence of our final results on the mass prescriptions for  $m_D$  and  $m_q$  is forthcoming in a longer paper.<sup>14)</sup>

#### §4. Results

In Fig. 1, we show the normalized pressure for  $N_c = 3$  and  $N_f = 2 + 1$  (left panel), and  $N_c = 3$  and  $N_f = 2 + 1 + 1$  (right panel) as a function of  $T$ . The results

at LO, NLO, and NNLO use the BN mass given by Eq. (3.4) as well as  $m_q = 0$ . For the strong coupling constant  $\alpha_s$ , we used three-loop running<sup>18)</sup> with  $\Lambda_{\overline{\text{MS}}} = 344$  MeV which for  $N_f = 3$  gives  $\alpha_s(5 \text{ GeV}) = 0.2034$ .<sup>19)</sup> The central line is evaluated with the renormalization scale  $\mu = 2\pi T$  which is the value one expects from effective field theory calculations<sup>9),20)</sup> and the band represents a variation of  $\mu$  by a factor of two around this scale.

The lattice data from the Wuppertal-Budapest collaboration uses the stout action and have been continuum extrapolated by averaging the trace anomaly measured using their two smallest lattice spacings corresponding to  $N_\tau = 8$  and  $N_\tau = 10$ .<sup>6)\*)</sup> Using standard lattice techniques, the continuum-extrapolated pressure is computed from an integral of the trace anomaly. The lattice data from the hotQCD collaboration are their  $N_\tau = 8$  results using both the asqtad and p4 actions.<sup>5)</sup> The hotQCD results have not been continuum extrapolated and the error bars correspond to only statistical errors and do not factor in the systematic error associated with the calculation which, for the pressure, is estimated by the hotQCD collaboration to be between 5 and 10%. We note that there are hotQCD results for physical light quark masses;<sup>21)</sup> however, these are available only for temperatures below 260 MeV and the results are very close to the results shown in the figures so we do not include them here.

As can be seen from Fig. 1 the successive HTLpt approximations represent an improvement over the successive approximations coming from a naive weak-coupling expansion; however, as in the pure-gluon case,<sup>17)</sup> the NNLO result represents a significant correction to the LO and NLO results. That being said the NNLO HTLpt result agrees quite well with the available lattice data down to temperatures on the order of  $2T_c \sim 340$  MeV for both  $N_f = 3$  (Fig. 1 left) and  $N_f = 4$  (Fig. 1 right). Below these temperatures the successive approximations give large corrections with the correction from NLO to NNLO reaching 100% near  $T_c$ .

In Fig. 2, we show the NNLO approximation to the trace anomaly (interaction measure) normalized to  $T^4$  as a function of  $T$  for  $N_c = 3$  and  $N_f = 3$  (left panel) and for  $N_c = 3$  and  $N_f = 4$  (right panel). In the left panel we show data from both the Wuppertal-Budapest collaboration and the hotQCD collaboration taken from the same data sets displayed in Fig. 1 and described previously. In the case of the hotQCD results we note that the results for the trace anomaly using the p4 action show large lattice size effects at all temperatures shown and the asqtad results for the trace anomaly show large lattice size effects for  $T \gtrsim 200$  MeV. In the right panel we display a parameterization (solid blue curve) of the trace anomaly for  $N_f = 4$  published by the Wuppertal-Budapest collaboration<sup>6)</sup> since the individual data points were not published. In both the left and right panels we see very good agreement with the available lattice data down to temperatures on the order of  $T \sim 2T_c$ .

---

\*) We note that the Wuppertal-Budapest group has published a few data points for the trace anomaly with  $N_\tau = 12$  and within statistical error bars these are consistent with the published continuum extrapolated results.

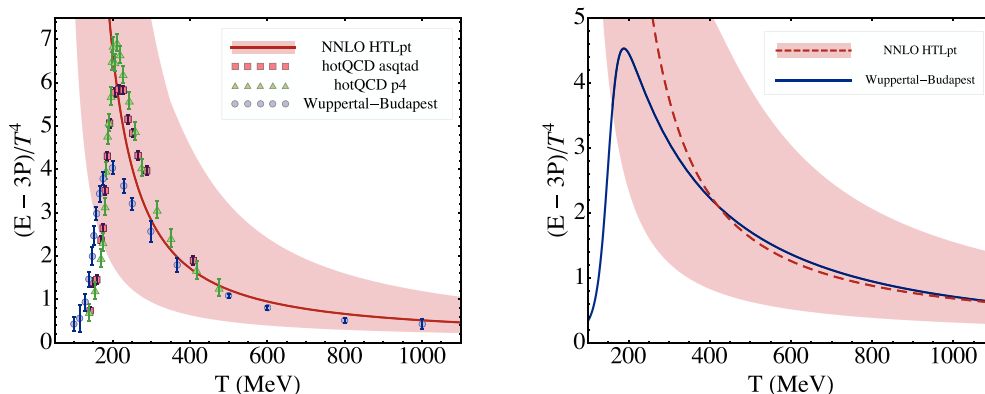


Fig. 2. Comparison of NNLO predictions for the scaled trace anomaly with  $N_f = 2 + 1$  (left panel) and  $N_f = 2 + 1 + 1$  fermions (right panel) lattice data from Cheng et al.<sup>5)</sup> and Borsanyi et al.<sup>6)</sup> We use  $N_c = 3$ , three-loop running for  $\alpha_s$ ,  $\mu = 2\pi T$ , and  $\Lambda_{\overline{\text{MS}}} = 344$  MeV. Shaded band shows the result of varying the renormalization scale  $\mu$  by a factor of two around  $\mu = 2\pi T$ . See main text for details.

## §5. Summary and outlook

We have reviewed recent results for the LO, NLO, and NNLO thermodynamic functions for  $SU(N_c)$  Yang-Mills theory with  $N_f$  fermions using HTLpt. We compared our predictions with lattice data for  $N_c = 3$  and  $N_f \in \{3, 4\}$  and found that HTLpt is consistent with available lattice data down to  $T \sim 2T_c$  for the pressure and the trace anomaly. This is in line with expectations since one is expanding about the trivial vacuum  $A_\mu = 0$  and therefore neglects the approximate center symmetry  $Z(N_c)$ . Close to the deconfinement transition, it is essential to incorporate this symmetry.<sup>22)</sup>

Comparing our results with the NNLO results of pure Yang-Mills,<sup>17)</sup> we find that including the quarks gives much better agreement with lattice data. This is not unexpected since fermions are “perturbative” in the sense that they decouple in the dimensional-reduction step of effective field theory.

As was the case with pure Yang-Mills we found that the variational solution for the Debye mass  $m_D$  is complex and we therefore chose instead to use the perturbative mass parameter from EQCD together with  $m_q = 0$ . Whether the complexity of the variational Debye mass is due to the additional expansion in  $m_D/T$  and  $m_q/T$  is impossible to decide at this stage. We also found that there was a large correction going from NLO to NNLO. Unfortunately, due to the magnetic mass problem it is impossible to go to N<sup>3</sup>LO to see whether the problem persists without supplementing our calculation with input from three-dimensional lattice calculations.

In closing, we emphasize that HTLpt provides a gauge invariant reorganization of perturbation theory for calculating static and dynamic quantities in thermal field theory. Given the good agreement with lattice data for thermodynamics, it would be interesting to apply HTLpt to the calculation of real-time quantities at temperatures that are relevant for LHC.

### Acknowledgments

M. Strickland would like to thank the Yukawa Institute for Theoretical Physics, Kyoto University, for their hospitality and for the invitation to present this work at the “High Energy Strong Interactions 2010” symposium. N. Su was supported by the Frankfurt International Graduate School for Science and Helmholtz Graduate School for Hadron and Ion Research. M. Strickland was supported by the Helmholtz International Center for FAIR LOEWE program.

### References

- 1) J. Adams *et al.* Nucl. Phys. A **757**, 102 (2005); K. Adcox *et al.*, *ibid.*, 184 (2005); I. Arsene *et al.*, *ibid.*, 1 (2005); B. B. Back *et al.*, *ibid.*, 28 (2005); M. Gyulassy and L. McLerran, Nucl. Phys. A **750**, 30 (2005).
- 2) G. Y. Qin, J. Ruppert, C. Gale, S. Jeon, G. D. Moore and M. G. Mustafa, Phys. Rev. Lett. **100**, 072301 (2008); G. Y. Qin and A. Majumder, arXiv:0910.3016 [hep-ph].
- 3) Z. Xu, C. Greiner and H. Stoecker, Phys. Rev. Lett. **101**, 082302 (2008).
- 4) J. O. Andersen, L. E. Leganger, M. Strickland, and N. Su, arXiv:1009.4644.
- 5) A. Bazavov *et al.*, Phys. Rev. D **80**, 014504 (2009).
- 6) S. Borsanyi *et al.*, arXiv:1007.2580 [hep-lat].
- 7) J. O. Andersen, E. Braaten and M. Strickland, Phys. Rev. D **61**, 074016 (2000); J. O. Andersen, E. Petitgirard and M. Strickland, Phys. Rev. D **70**, 045001 (2004).
- 8) E. V. Shuryak, Sov. Phys. JETP **47** (1978) 212 [Zh. Eksp. Teor. Fiz. **74**, 408 (1978)]; J. I. Kapusta, Nucl. Phys. B **148** (1979) 461; T. Toimela, Int. J. Theor. Phys. **24**, 901(1985) [Erratum-*ibid.* **26**, 1021 (1987)]; P. B. Arnold and C. X. Zhai, Phys. Rev. D **50**, 7603 (1994); Phys. Rev. D **51**, 1906 (1995); Phys. Rev. D **53**, 3421 (1996); C. X. Zhai and B. Kastening, Phys. Rev. D **52**, 7232 (1995); K. Kajantie, M. Laine, K. Rummukainen and Y. Schroder, Phys. Rev. D **67**, 105008 (2003).
- 9) E. Braaten and A. Nieto, Phys. Rev. Lett. **76**, 1417 (1996); Phys. Rev. D **53**, 3421 (1996).
- 10) J. P. Blaizot, E. Iancu and A. Rebhan, In *Hwa, R.C. (ed.) et al.: Quark gluon plasma*, 60-122, (2003); U. Kraemmer and A. Rebhan, Rept. Prog. Phys. **67**, 351 (2004); J. O. Andersen and M. Strickland, Annals Phys. **317**, 281 (2005).
- 11) F. Karsch, A. Patkos and P. Petreczky, Phys. Lett. B **401**, 69 (1997); S. Chiku and T. Hatsuda, Phys. Rev. D **58**, 076001 (1998); J. O. Andersen, E. Braaten and M. Strickland, Phys. Rev. D **63**, 105008 (2001); J. O. Andersen and M. Strickland, Phys. Rev. D **64** (2001) 105012; J. O. Andersen and L. Kyllingstad, Phys. Rev. D **78**, 076008 (2008).
- 12) W. Buchmüller and O. Philipsen, Nucl. Phys. B **443**, 47 (1995); G. Alexanian and V. P. Nair, Phys. Lett. B **352**, 435 (1995).
- 13) E. Braaten and R. D. Pisarski, Phys. Rev. D **45**, R1827 (1992); S. Mrowczynski, A. Rebhan, M. Strickland, Phys. Rev. **D70**, 025004 (2004).
- 14) J. O. Andersen, L. E. Leganger, M. Strickland, and N. Su, forthcoming.
- 15) A. D. Linde, Phys. Lett. B **96**, 289 (1980); D. J. Gross, R. D. Pisarski, L. G. Yaffe, Rev. Mod. Phys. **53**, 43 (1981).
- 16) J. O. Andersen, M. Strickland and N. Su, Phys. Rev. D **80**, 085015 (2009).
- 17) J. O. Andersen, M. Strickland, and N. Su, Phys. Rev. Lett. **104**, 122003 (2010); JHEP **1008**, 113 (2010).
- 18) C. Amsler *et al.* (Particle Data Group), Physics Letters B **667**, 1 (2008).
- 19) C. McNeile, C. T. H. Davies, E. Follana, K. Hornbostel and G. P. Lepage, Phys. Rev. D **82**, 034512 (2010).
- 20) M. Laine and Y. Schroder, Phys. Rev. D **73**, 085009 (2006).
- 21) M. Cheng *et al.*, Phys. Rev. D **81**, 054504 (2010).
- 22) C. Korthals-Altes, A. Kovner, and M. A. Stephanov, Phys. Lett. B **469**, 205 (1999) 205; R. D. Pisarski, Phys. Rev. D **62**, 111501 (2000); A. Vuorinen and L. G. Yaffe, Phys. Rev. D **74**, 025011 (2006); Ph. de Forcrand, A. Kurkela, and A. Vuorinen, Phys. Rev. D **77**, 125014 (2008); Y. Hidaka and R. D. Pisarski, Phys.Rev. **D80**, 036004 (2009).